Dyes and Pigments 88 (2011) 88–94

Contents lists available at ScienceDirect

Dyes and Pigments

journal homepage: www.elsevier.com/locate/dyepig

The synthesis, crystal structure and photophysical properties of mononuclear platinum(II) 6-phenyl-[2,2′]bipyridinyl acetylide complexes

Rui Liu, Jin Chang, Qi Xiao, Yuhao Li, Hongbin Chen, Hongjun Zhu*

Department of Applied Chemistry, College of Science, Nanjing University of Technology, Nanjing 210009, PR China

ARTICLE INFO

Article history:
Received 18 January 2010
Received in revised form
10 May 2010
Accepted 10 May 2010
Available online 19 May 2010

Keywords:
Cyclometalated Pt(II) complexes
Phenylacetylide
Bipyridyl
Crystal structures
Photophysical property
Organic light-emitting diodes (OLEDs)

ABSTRACT

The synthesis, structural, electrochemical and photophysical properties of a series of 4,6-diphenyl-2,2′-bipyridine platinum(II) complexes bearing σ-alkynyl ancillary ligands were studied. Absorption bands were observed in UV–Vis absorption spectra (maximum peaks range from 431 to 455 nm) and phosphorescence emission maxima varied from 554 nm to 577 nm. Both the UV absorption and photoluminesence emission maxima of the complexes were red-shifted in accordance with not only the electron-donating ability of the *para*-substituent on the phenylacetylide ligand, but also the extension of the π-conjugated length of the oligo phenylacetylide ligand. The photoluminescent and electrochemical properties as well as crystal structure were investigated with the aim of providing the basis for elucidating structure-physical property relationships in the context of light-emitting materials.

1. Introduction

Cyclometalated square-planar platinum(II) complexes have attracted a great deal of attention owing to their use in optoelectronic devices, chemosensors, photovoltaic cells and photocatalysis [1–10]. The square-planar Pt(II) coordination geometry discourages D_{2d} distortion which is likely to result in radiationless decay and their photophysical properties can be modulated by structurally modifying the ligands employed [11,12]. Of these, square-planar platinum(II) σ-alkynyl complexes have been extensively investigated and in the context of organic light-emitting diodes (OLEDs), nonlinear optical materials, low-dimension conductors and photovoltaic devices by virtue of their chemical and structural stability [13–19]. As rigid π-conjugated bridging components of these complexes, acetylide moieties facilitate a wide range of photorelated processes, including triplet energy transfer, electron (or hole) transfer, photon migration, and electron delocalization, while maintaining strict stereochemical integrity.

Che and co-workers [13,14] synthesized a series of 6-aryl-2,2′-bypyridine tridentate cyclometalated platinum(II) complexes containing σ-alkynyl auxiliaries, and showed that the σ-alkynyl component can act as photophysically 'active' ligand which constitutes an integral part of the electronic structure through Pt-(alkynyl) π-conjugation. Additionally, the anionic σ-alkynyl ligand lends neutrality to the [Pt(C^N^N)] moiety and is envisaged to modulate their photophysical properties by measn of variation of the substituent in the acetylide moiety. The metal-to-ligand charge transfer (^{1}MLCT) absorption band and the emission maximum of the complexes can be systematically altered in accordance with the electron-donating or electron- withdrawing ability of the *para*-substituent in the phenylacetylide ligand. In this context, the development of novel, tridentate, cyclometalated platinum(II) complexes containing various σ-alkynyl moieties and their photophysical properties and structure-property relationships are feasible, challengeable and potentially valuable.

This paper concerns a series of novel, mononuclear platinum(II) 6-phenyl-[2,2′]bipyridinyl acetylide complexes, that contain various arylacetylide substituents (Scheme 1). Their photophysical properties were investigated with the aim of understanding structure-physical property relationships in the context of novel organic light-emitting materials.

2. Experimental

2.1. Materials

All reagents were purchased from Sinopharm Chemcial Reagent Co. Ltd. Dichloromethane, chloroform and acetonitrile were

* Corresponding author. Tel.: +86 25 83172358; fax: +86 25 83587443.
E-mail address: zhuhjnjut@hotmail.com (H. Zhu).

0143-7208/$ – see front matter © 2010 Elsevier Ltd. All rights reserved.
doi:10.1016/j.dyepig.2010.05.005

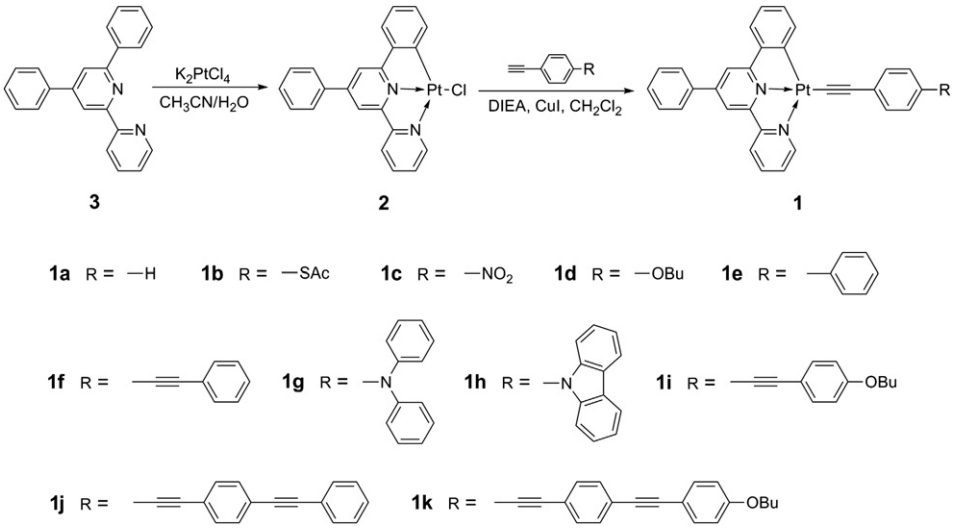

Scheme 1. Synthesis of Pt(II) complexes (**1a**–**1k**).

purified by redistillation. Tetrahydrofuran (THF) and *N,N*-diisopropylethylamine (DIEA) were distilled under N_2 over sodium benzophenone ketyl. Tetra-*n*-butylammonium perchlorate (TBAP) and ferrocene were purified by recrystallization twice from ethanol. All other reagents were used as received. 4,6-Diphenyl-2,2′-bipyridine (**3**) [13] and phenylacetylide ligands [20–25] were synthesized according to literature methods.

2.2. Measurements

^{1}H NMR and ^{13}C NMR spectra were recorded on either a Bruker AV-500 or AV-300 spectrometer using DMSO-d_6 as the solvent, with tetramethylsilane as internal standard. The elemental analyses were performed with a Vario El III elemental analyzer. High resolution mass (HRMS) analyses were performed at an AutoSpec Premier mass spectrometer (Waters). Optical absorption spectra were obtained by using a Cary 5000 UV/Spectrophotometer (Varian). PL spectra were carried out on a LS-55 spectrofluorometer (Perkin-Elmer). The X-ray crystallographic analysis was performed on a Nonius CAD4 single-crystal diffractometer. The electrochemical experiments were carried out using a CHI 660C electrochemistry workstation (CHI USA). A standard one-compartment three-electrode cell was used with a Pt electrode as the working electrode, a Pt wire as the counter electrode and a Ag/Ag$^+$ electrode (Ag in 0.1 M $AgNO_3$ solution, from CHI, Inc) as the reference electrode. TBAP (0.1 M) was used as the supporting electrolyte and the scan rate was 100 mV s^{-1}.

2.3. Synthesis

2.3.1. Synthesis of complex (C^N^N)PtCl (**2**)

4,6-Diphenyl-2,2′-bipyridyl (0.31 g, 1.0 mmol, 1.0 equiv.), K_2PtCl_4 (0.41 g, 1.0 mmol, 1.0 equiv.), acetonitrile and water (v/v = 1:1, 40 mL) were mixed in a round-bottom flask and refluxed for 48 h under a dry atmosphere of N_2. The mixture was cooled to ambient and filtered; the precipitate was rinsed with acetonitrile (20 mL) and water (20 mL) to afford 0.33 g orange solid complex **2** in 61.0% yield [13]. ^{1}H NMR (DMSO-d_6, 300 MHz): δ ppm 8.92 (d, J = 5.1 Hz, 1H), 8.76 (d, J = 8.0 Hz, 1H), 8.53 (s, 1H), 8.38 (t, J = 7.8 Hz, 1H), 8.28 (s, 1H), 8.12 (d, J = 6.8 Hz, 2H), 7.93 (d, J = 7.3 Hz, 1H), 7.83 (d, J = 7.5 Hz, 1H), 7.61–7.50 (m, 4H), 7.18–7.07 (m, 2H).

2.3.2. General procedure for synthesis of complexes ***1a*–*1k***

A mixture of **2** (0.54 g, 1 mmol, 1.0 equiv.), phenylacetylide (3 mmol, 3.0 equiv.), DIEA (0.45 g, 3.5 mmol, 3.5 equiv.) and CuI (0.019 g, 10 mol %) in degassed CH_2Cl_2 (30 mL) was stirred for 12 h under a nitrogen atmosphere at room temperature in the absence of light. The mixture was then quenched with water, extracted with CH_2Cl_2 (3 × 30 mL). The organic layer was washed with water (50 mL), dried over anhydrous magnesium sulfate and evaporated to dryness. Then the crude product was purified by recrystallization from CH_2Cl_2/Et_2O (v/v = 3:1, 20 mL) to afford to give the desired product.

*2.3.2.1. Complex [(C^N^N)PtC≡CC_6H_5] (**1a**).* Yield was 62.1% as orange solid [11]. ^{1}H NMR (DMSO-d_6, 300 MHz): δ ppm 9.10 (d, J = 4.5 Hz, 1H), 8.77 (d, J = 8.2 Hz, 1H), 8.59 (s, 1H), 8.40 (t, J = 7.2 Hz, 1H), 8.35 (s, 1H), 8.12 (d, J = 8.0 Hz, 2H), 7.92–7.89 (m, 2H), 7.79 (d, J = 6.5 Hz, 1H), 7.63–7.60 (m, 3H), 7.38 (d, J = 7.4 Hz, 2H), 7.29 (t, J = 7.5 Hz, 2H), 7.19–7.09 (m, 3H).

*2.3.2.2. Complex [(C^N^N)PtC≡CC_6H_4-4-SAc] (**1b**).* Yield was 58.8% as orange solid. ^{1}H NMR (DMSO-d_6, 300 MHz): δ ppm 9.05 (d, J = 5.5 Hz, 1H), 8.75 (d, J = 8.1 Hz, 1H), 8.58 (s, 1H), 8.38 (t, J = 7.2 Hz, 1H), 8.33 (s, 1H), 8.11 (d, J = 6.0 Hz, 2H), 7.88 (t, J = 6.6 Hz, 2H), 7.75 (d, J = 7.1 Hz, 1H), 7.60–7.62 (m, 3H), 7.43 (d, J = 8.2 Hz, 2H), 7.32 (t, J = 8.2 Hz, 2H), 7.14–7.09 (m, 2H), 2.43 (s, 3H). ^{13}C NMR (DMSO-d_6, 300 MHz): δ ppm 193.8, 164.3, 157.4, 154.7, 151.3, 142.2, 140.1, 137.6, 136.5, 134.2, 131.7, 130.2, 130.1, 129.0, 128.7, 127.6, 125.4, 124.4, 123.6, 123.3, 117.0, 116.4, 30.0. HRMS *m/z* [M]$^+$ Calcd. for $C_{32}H_{22}N_2OPtS$: 677.1101. Found: 677.1098. Anal. Calcd. (%) for $C_{32}H_{22}N_2OPtS$: C, 56.72; H, 3.27; N, 4.13. Found: C, 56.69; H, 3.30; N, 4.12.

*2.3.2.3. Complex [(C^N^N)PtC≡CC_6H_4-4-NO_2] (**1c**).* Yield was 63.3% as orange solid. ^{1}H NMR (DMSO-d_6, 300 MHz): δ ppm 9.02 (d, J = 4.5 Hz, 1H), 8.76 (d, J = 7.6 Hz, 1H), 8.59 (s, 1H), 8.39 (t, J = 8.2 Hz, 1H), 8.25 (d, J = 8.5 Hz, 1H), 8.17 (s, 1H), 8.14–8.10 (m, 3H), 7.8 (s, 2H), 7.71 (d, J = 7.2 Hz, 1H), 7.62–7.56 (m, 5H), 7.14–7.09 (m, 2H). ^{13}C NMR (DMSO-d_6, 300 MHz): δ ppm 165.2, 158.3, 156.6, 154.3, 151.5, 151.3, 146.8, 142.6, 138.6, 138.5, 137.3, 132.9, 131.1, 129.8, 129.4, 127.3, 124.5, 123.6, 122.4, 121.5, 117.5, 116.2, 114.2, 105.5. HRMS *m/z* [M]$^+$ Calcd. for $C_{30}H_{19}N_3O_2Pt$: 648.1125. Found: 648.1103. Anal. Calcd. (%) for $C_{30}H_{19}N_3O_2Pt$: C, 55.56; H, 2.95; N, 6.48. Found: C, 55.51; H, 2.99; N, 6.44.

*2.3.2.4. Complex [(C^N^N)PtC≡CC$_6$H$_4$-4-OBu] (**1d**).* Yield was 68.8% as orange solid. ^{1}H NMR (DMSO-d_6, 300 MHz): δ ppm 9.18 (d, J = 4.5 Hz, 1H), 8.76 (d, J = 7.8 Hz, 1H), 8.61 (s, 1H), 8.42 (t, J = 8.2 Hz, 1H), 8.35 (s, 1H), 8.11 (d, J = 7.2 Hz, 2H), 7.88–7.94 (m, 2H), 7.78 (d, J = 7.7 Hz, 1H), 7.63–7.58 (m, 3H), 7.46 (d, J = 8.7 Hz, 2H), 7.15–7.09 (m, 2H), 6.83 (d, J = 8.7 Hz, 2H), 3.98 (t, J = 6.4 Hz, 2H), 1.80–1.75 (m, 2H), 1.53–1.47 (m, 2H), 0.98 (t, J = 7.3 Hz, 3H). ^{13}C NMR (DMSO-d_6, 300 MHz): δ ppm 165.1, 158.0, 156.9, 154.4, 151.3, 151.1, 146.7, 142.4, 138.5, 138.2, 137.2, 132.8, 131.0, 129.7, 129.2, 127.1, 124.4, 123.3, 122.8, 121.3, 116.4, 116.2, 114.1, 105.8, 67.7, 31.4, 19.2, 13.8. HRMS m/z [M]$^+$ Calcd. for $C_{34}H_{28}N_2OPt$: 675.1849. Found: 675.1838. Anal. Calcd. (%) for $C_{34}H_{28}N_2OPt$: C, 60.44; H, 4.18; N, 4.15. Found: C, 60.40; H, 4.21; N, 4.11.

*2.3.2.5. Complex [(C^N^N)PtC≡CC$_6$H$_4$-4-C$_6$H$_4$] (**1e**).* Yield was 65.1% as orange solid. ^{1}H NMR (DMSO-d_6, 500 MHz): δ ppm 9.10 (d, J = 4.6 Hz, 1H), 8.76 (d, J = 8.1 Hz, 1H), 8.58 (s, 1H), 8.39 (t, J = 7.8 Hz, 1H), 8.34 (s, 1H), 8.11 (d, J = 6.8 Hz, 2H), 7.91–7.86 (m, 2H), 7.80 (d, J = 7.3 Hz, 1H), 7.68 (d, J = 7.3 Hz, 2H), 7.64–7.57 (m, 5H), 7.48–7.45 (m, 4H), 7.35 (t, J = 7.3 Hz, 1H), 7.17–7.08 (m, 2H). ^{13}C NMR (DMSO-d_6, 300 MHz): δ ppm 157.6, 154.6, 151.2, 147.2, 142.3, 140.0, 137.5, 136.5, 131.6, 130.6, 130.2, 129.1, 128.8, 128.6, 127.5, 127.0, 126.2, 126.1, 125.3, 123.5, 117.0, 116.4. HRMS m/z [M]$^+$ Calcd. for $C_{36}H_{24}N_2Pt$: 679.1587. Found: 679.1579. Anal. Calcd. (%) for $C_{36}H_{24}N_2Pt$: C, 63.62; H, 3.56; N, 4.12. Found: C, 63.39; H, 3.60; N, 4.08.

*2.3.2.6. Complex [(C^N^N)Pt(C≡CC$_6$H$_4$C≡CC$_6$H$_5$)] (**1f**).* Yield was 63.2% as orange solid. ^{1}H NMR (DMSO-d_6, 500 MHz): δ ppm 9.07 (d, J = 4.5 Hz, 1H), 8.77 (d, J = 8.0 Hz, 1H), 8.59 (s, 1H), 8.40 (t, J = 7.1 Hz, 1H), 8.34 (s, 1H), 8.12 (d, J = 6.8 Hz, 2H), 7.91–7.87 (m, 2H), 7.77 (d, J = 7.4 Hz, 1H), 7.64–7.55 (m, 6H), 7.47–7.42 (m, 6H), 7.16 (t, J = 7.3 Hz, 1H), 7.10 (t, J = 7.3 Hz, 1H). ^{13}C NMR (DMSO-d_6, 300 MHz): δ ppm 157.2, 154.1, 151.0, 142.7, 141.0, 132.9, 132.3, 131.6, 129.3, 128.7, 127.5, 127.1, 125.6, 122.5, 122.3, 117.8, 116.2, 93.8, 89.2. HRMS m/z [M]$^+$ Calcd. for $C_{38}H_{24}N_2Pt$: 703.1587. Found: 703.1580. Anal. Calcd. (%) for $C_{38}H_{24}N_2Pt$: C, 64.86; H, 3.44; N, 3.98. Found: C, 64.82; H, 3.47; N, 4.00.

*2.3.2.7. Complex [(C^N^N)PtC≡CC$_6$H$_4$-4-N(C$_6$H$_4$)$_2$] (**1g**).* Yield was 66.7% as orange solid. ^{1}H NMR (DMSO-d_6, 500 MHz): δ ppm 9.07 (d, J = 5.3 Hz, 1H), 8.76 (d, J = 7.9 Hz, 1H), 8.58 (s, 1H), 8.38 (t, J = 7.1 Hz, 1H), 8.33 (s, 1H), 8.11 (d, J = 6.6 Hz, 2H), 7.90–7.85 (m, 2H), 7.78 (d, J = 7.6 Hz, 1H), 7.63–7.57 (m, 3H), 7.44 (d, J = 8.0 Hz, 1H), 7.35–7.29 (m, 6H), 7.14 (t, J = 7.3 Hz, 1H), 7.08 (t, J = 7.3 Hz, 1H), 7.03–7.01 (m, 4H), 6.95–6.91 (m, 3H). ^{13}C NMR (DMSO-d_6, 300 MHz): δ ppm 157.4, 154.9, 151.0, 145.8, 145.6, 142.7, 139.3, 131.7, 129.6, 129.3, 127.7, 127.0, 126.8, 125.6, 125.3, 123.5, 122.9, 122.4, 117.8, 116.2. HRMS m/z [M]$^+$ Calcd. for $C_{42}H_{29}N_3Pt$: 770.2009. Found: 770.1998. Anal. Calcd. (%) for $C_{42}H_{29}N_3Pt$: C, 65.45; H, 3.79; N, 5.45. Found: C, 65.42; H, 3.83; N, 5.41.

*2.3.2.8. Complex [(C^N^N)PtC≡CC$_6$H$_4$-4-(9-Carbazole)] (**1h**).* Yield was 65.9% as orange solid. ^{1}H NMR (DMSO-d_6, 500 MHz): δ ppm 9.15 (d, J = 4.5 Hz, 1H), 8.79 (d, J = 8.1 Hz, 1H), 8.62 (s, 1H), 8.42 (t, J = 7.1 Hz, 1H), 8.37 (s, 1H), 8.25 (d, J = 7.8 Hz, 2H), 8.12 (d, J = 6.8 Hz, 2H), 7.93–7.89 (m, 2H), 7.84 (d, J = 7.3 Hz, 1H), 7.67-7.60 (m, 5H), 7.53 (d, J = 8.6 Hz, 2H), 7.48–7.42 (m, 4H), 7.30 (t, J = 7.3 Hz, 2H), 7.18 (t, J = 7.3 Hz, 1H), 7.13 (t, J = 7.3 Hz, 1H). ^{13}C NMR (DMSO-d_6, 300 MHz): δ ppm 157.3, 154.4, 151.2, 145.6, 145.3, 142.7, 139.3, 131.4, 129.8, 129.3, 127.7, 127.2, 126.8, 125.5, 125.4, 123.5, 122.8, 122.4, 117.8, 116.5. HRMS m/z [M]$^+$ Calcd. for $C_{42}H_{27}N_3Pt$: 768.1853. Found: 768.1847. Anal. Calcd. (%) for $C_{42}H_{27}N_3Pt$: C, 65.62; H, 3.54; N, 5.47. Found: C, 65.64; H, 3.58; N, 5.43.

*2.3.2.9. Complex [(C^N^N)Pt(C≡CC$_6$H$_4$C≡CC$_6$H$_4$)-4-OBu] (**1i**).* Yield was 64.5% as orange solid. ^{1}H NMR (DMSO-d_6, 500 MHz): δ 9.08 (d, J = 4.5 Hz, 1H), 8.77 (d, J = 7.9 Hz, 1H), 8.60 (s, 1H), 8.40 (t, J = 8.2 Hz, 1H), 8.35 (s, 1H), 8.12 (d, J = 7.1 Hz, 2H), 7.93–7.89 (m, 2H), 7.78 (d, J = 7.7 Hz, 1H), 7.62–7.59 (m, 3H), 7.47 (d, J = 8.8 Hz, 2H), 7.44–7.39 (m, 4H), 7.16–7.10 (m, 2H), 6.97 (d, J = 8.8 Hz, 2H), 4.01 (t, J = 6.4 Hz, 2H), 1.72–1.69 (m, 2H), 1.47–1.42 (m, 2H), 0.94 (t, J = 7.5 Hz, 3H). ^{13}C NMR (DMSO-d_6, 300 MHz): δ ppm 157.4, 154.2, 151.8, 142.2, 141.5, 132.4, 132.3, 131.6, 129.7, 128.3, 127.7, 127.3, 125.8, 122.4, 122.1, 117.5, 116.7, 93.4, 89.6, 67.6, 31.2, 19.6, 13.9. HRMS m/z [M]$^+$ Calcd. for $C_{42}H_{32}N_2OPt$: 775.2162. Found: 775.2155. Anal. Calcd. (%) for $C_{42}H_{32}N_2OPt$: C, 65.02; H, 4.16; N, 3.61. Found: C, 64.98; H, 4.20; N, 3.59.

*2.3.2.10. Complex [(C^N^N)Pt(C≡CC$_6$H$_4$C≡CC$_6$H$_4$C≡CC$_6$H$_5$)] (**1j**).* Yield was 59.1% as orange solid. ^{1}H NMR (DMSO-d_6, 500 MHz): δ ppm 9.07 (d, J = 4.5 Hz, 1H), 8.76 (d, J = 8.0 Hz, 1H), 8.60 (s, 1H), 8.42 (t, J = 7.2 Hz, 1H), 8.36 (s, 1H), 8.11 (d, J = 6.8 Hz, 2H), 7.93–7.89 (m, 2H), 7.85 (d, J = 7.4 Hz, 1H), 7.66–7.61 (m, 10H), 7.51–7.44 (m, 6H), 7.18–7.08 (m, 2H). ^{13}C NMR (DMSO-d_6, 300 MHz): δ ppm 157.4, 154.2, 151.0, 142.6, 141.1, 132.9, 132.6, 131.3, 129.4, 128.7, 127.5, 127.4, 125.6, 122.6, 122.3, 117.6, 116.3, 93.8, 93.7, 89.2, 89.0. HRMS m/z [M]$^+$ Calcd. for $C_{46}H_{28}N_2Pt$: 803.1900. Found: 803.1894. Anal. Calcd. (%) for $C_{46}H_{28}N_2Pt$: C, 68.73; H, 3.51; N, 3.49. Found: C, 68.70; H, 3.54; N, 3.47.

*2.3.2.11. Complex [(C^N^N)Pt(C≡CC$_6$H$_4$C≡CC$_6$H$_4$C≡CC$_6$H$_4$)-4-OBu] (**1k**).* Yield was 60.4% as orange solid. ^{1}H NMR (DMSO-d_6, 500 MHz): δ ppm 9.37 (d, J = 4.6 Hz, 1H), 8.76 (d, J = 8.1 Hz, 1H), 8.56 (s, 1H), 8.35 (t, J = 7.2 Hz, 1H), 8.30 (s, 1H), 8.12 (d, J = 6.8 Hz, 2H), 7.88–7.83 (m, 3H), 7.62–7.60 (m, 6H), 7.85 (d, J = 7.4 Hz, 4H), 7.44–7.42 (m, 4H), 7.14–7.08 (m, 2H), 6.97 (d, J = 8.8 Hz, 2H), 4.01 (t, J = 6.4 Hz, 2H), 1.72–1.68 (m, 2H), 1.46–1.40 (m, 2H), 0.94 (t, J = 7.5 Hz, 3H). ^{13}C NMR (DMSO-d_6, 300 MHz): δ ppm 157.2, 154.4, 151.8, 142.1, 141.6, 132.8, 132.6, 131.5, 129.4, 128.3, 127.8, 127.3, 125.4, 122.3, 122.0, 117.1, 116.7, 93.3, 89.5, 67.6, 31.0, 19.7, 13.6. HRMS m/z [M]$^+$ Calcd. for $C_{50}H_{36}N_2OPt$: 875.2475. Found: 875.2467. Anal. Calcd. (%) for $C_{50}H_{36}N_2OPt$: C, 68.56; H, 4.14; N, 3.20. Found: C, 68.53; H, 4.17; N, 3.18.

2.4. X-ray diffraction crystallography

Crystals of **1b** suitable for single crystal X-ray diffraction were obtained by slow diffusion of diethyl ether into a dichloromethane solution of the complex. The diffraction data were collected on a Nonius CAD4 single crystal diffractometer equipped with a graphite-monochromated Mo$K\alpha$ radiation (λ = 0.71073 Å) by using an $\omega/2\theta$ scan mode at 296 K. The crystal structures were solved by the direct method and refined by the full-matrix least-squares procedure on F^2 using SHELXL-97 program [26]. All non-hydrogen atoms were refined anisotropically, and the hydrogen atoms were introduced at calculated positions. The crystal and structure refinement data of **1b** are listed in Table 1.

3. Results and discussions

3.1. Synthesis and characterization

Scheme 1 outlines the synthesis of the platinum(II) 6-phenyl-[2,2‘]bipyridinyl acetylide complexes. Pt(II) acetylide complexes derived from these precursors were prepared by employing Sonogashira’s conditions (terminal alkynes, CuI/^{i}Pr$_2$NH/CH$_2$Cl$_2$) and were obtained in 58–68% yield after recrystallization. All complexes are air-stable and soluble in CH_2Cl_2, $CHCl_3$, acetone, tetrahydrofuran, and dimethyl sulphoxide, except **1f** and **1j** which

Table 1
Crystal and structure refinement data of complex **1b**.

Chemical formula	$C_{32}H_{22}N_2OPtS$	θ range (°)	2.21–27.52
Formula weight	677.67	Index range	$-21 \le h \le 21$
Crystal system	Monoclinic		$-9 \le k \le 9$
Space group	$P2_1/c$		$-26 \le l \le 26$
a (Å)	16.933 (9)	Reflns collected	21070
b (Å)	7.315 (4)	Unique reflns (R_{int})	5863 (0.077)
c (Å)	20.807 (12)	Refinement mothod on F^2	Full-matrix least-squares
α (°)	90	GOF on F^2	1.037
β (°)	95.560 (8)	R_1 [$I > 2\sigma$ (I)]	0.0372
γ (°)	90	wR_2 [$I > 2\sigma$ (I)]	0.0778
V (Å^3), Z	2565 (2)/4	R_1 (all data)	0.0753
D_{calc} (g cm^{-3})	1.755	wR_2 (all data)	0.0953
μ (mm^{-1})	5.581	Residual (e Å^{-3})	1.977 and −1.115
F (0 0 0)	1320		

Table 2
Selected bond length (Å) and angles (°) for complex **1b**.

C9–N1	1.367(8)	C28–S1	1.775(6)
C10–N1	1.345(8)	C31–O1	1.203(9)
C17–Pt1	2.088(6)	C31–S1	1.766(10)
C18–N2	1.402(8)	N1–Pt1	1.989(5)
C22–N2	1.364(8)	N2–Pt1	2.083(6)
C23–Pt1	1.997(6)		
N1–C9–C8	119.5(6)	C32–C31–S1	113.2(7)
N1–C9–C18	113.1(5)	C10–N1–C9	122.3(5)
N1–C10–C11	119.7(6)	C10–N1–Pt1	119.6(4)
N1–C10–C12	112.4(5)	C9–N1–Pt1	118.1(4)
C16–C17–Pt1	129.7(5)	C22–N2–C18	119.8(6)
C12–C17–Pt1	112.2(4)	C22–N2–Pt1	128.2(5)
C19–C18–N2	119.9(6)	C18–N2–Pt1	111.8(4)
N2–C18–C9	116.4(6)	N1–Pt1–C23	177.2(2)
N2–C22–C21	120.5(6)	N1–Pt1–N2	80.5(2)
C24–C23–Pt1	173.3(6)	C23–Pt1–N2	97.9(2)
C27–C28–S1	120.3(6)	N1–Pt1–C17	79.8(2)
C29–C28–S1	119.2(5)	C23–Pt1–C17	101.9(2)
O1–C31–C32	122.5(9)	N2–Pt1–C17	160.1(2)
O1–C31–S1	124.3(6)	C31–S1–C28	102.4(4)

display low solubility in common organic solvents. ^{1}H NMR spectra, ^{13}C NMR spectra, HRMS and elemental analysis confirmed the proposed structures. The NMR data for all of the complexes are consistent with the assigned structures and previously reported complexes of this type [13–15]. All of the complexes have distinct, well-resolved patterns in their aromatic proton resonances, which are attributable to the protons of the pyridine rings and phenyl substituents. The pyridine resonances (δ 7.8–9.4 ppm) are particularly informative, as they shift substantially upon coordination of the Pt(II) metal ion and upon exchange of chloride for acetylide, particularly the protons nearest the acetylide moiety. In addition, the structure of complex **1b** was revealed by X-ray crystallography.

3.2. Crystal structure of complex *1b*

The perspective view and the packing diagram of complex **1b** are shown in Fig. 1. Selected bond distances and angles are listed in Table 2. The coordinate geometry of the Pt atom is a distorted square planar configuration with a C(17)–Pt(1)–N(2) angle of 160.1°. The bond distances of Pt–N(1) and Pt–N(2) are 1.989(5) and 2.083(6) Å, respectively, which are comparable to those of previously reported analogous [12,15,19]. The acetylenic units have alternating C≡C and C–C distances and deviate slightly from linear

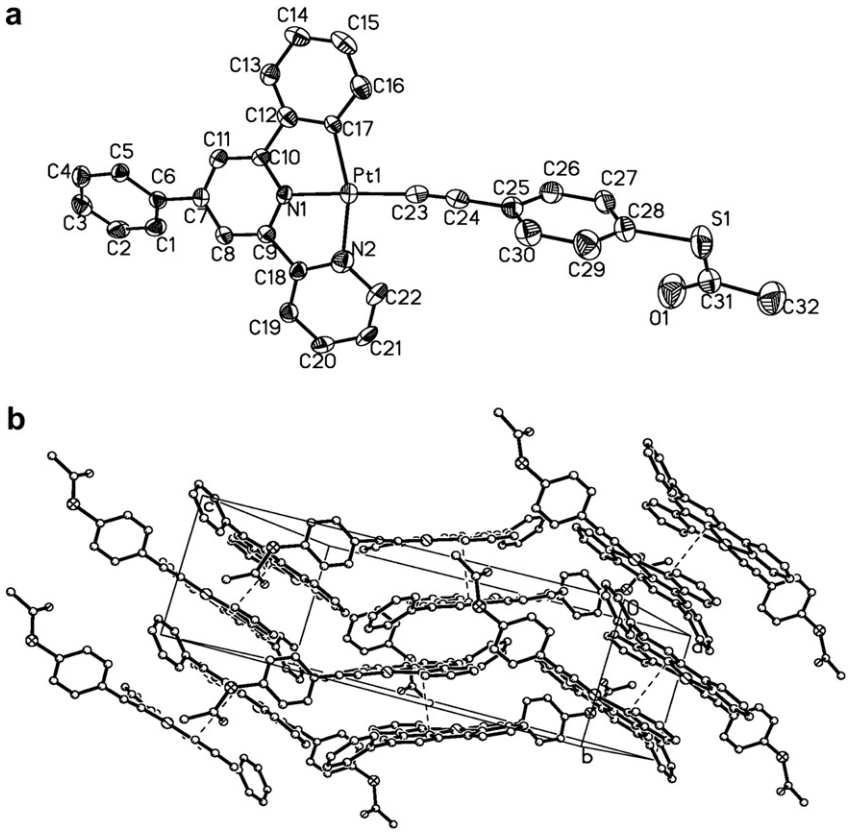

Fig 1. Single crystal structure (a) and the packing diagram (b) of **1b**, the intermolecular π-stacking interactions are shown as dashed lines.

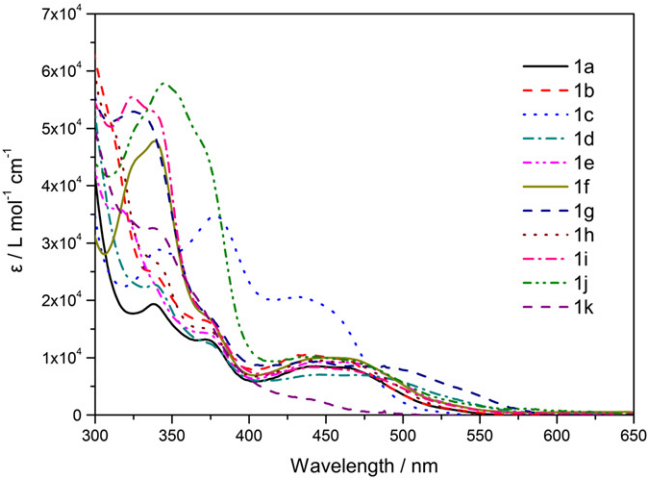

Fig 2. UV–Vis absorption spectra of Pt(II) complexes in CH_2Cl_2 solution (10^{-5} M).

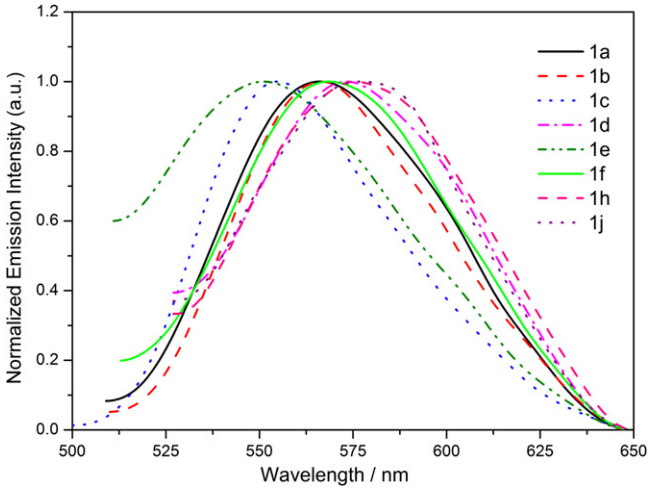

Fig 3. Emission spectra of Pt(II) complexes in CH_2Cl_2 solution (10^{-5} M).

geometry, as indicated by the angles at the acetylenic carbon atoms (174.3°). The dihedral angle between the phenyl ring at the 4-position of the C^N^N ligand and the plane of the [(C^N^N)Pt] moiety is 142.8°. The dihedral angle between the acetylenic phenyl ring and the plane of the [(C^N^N)Pt] moiety is 68.5°.

In the crystal structure of complex **1b**, there exists infinite stacks of complexes that have weak $\pi\ldots\pi$ interaction with interplanar distance in the range of 3.3–3.4 Å. The $\pi\ldots\pi$ stacking involves the phenyl ring of the C^N^N ligand from one molecule and the central pyridine ring of the C^N^N ligand in a nearest-neighbor molecule. The intermolecular Pt…Pt distance of 4.77 Å is suggestive of no metal–metal interaction.

3.3. Optical properties

The UV–Vis absorption spectra of complexes **1a**–**1k** in CH_2Cl_2 solution (10^{-5} M) at 298 K are shown in Fig. 2, and the optical characteristics are summarized in Table 3. With reference to previous work [11,15] on cyclometalated platinum(II) complexes, the absorption bands of <370 nm are assigned to a serials of intra-ligand (IL) charge-transfer transitions, while the absorption bands at 400–550 nm are assigned to the ^{1}MLCT transitions. These low-energy absorption peak maxima appear at 431 to 455 nm and systematically red-shift in accordance with the electron-donating ability of the *para*-substituent on the phenylacetylide ligand. For **1c**, there is an additional intense absorption band at λ_{max} 378 nm ($\varepsilon \approx 3.5 \times 10^4$ dm^3 mol^{-1} cm^{-1}), which is characteristic of the ^{1}IL-(4-nitrophenylacetylide) charge-transfer transition [13]. The ^{1}MLCT absorption band obeys Beer's law in the range from 10^{-5} to 10^{-4} mol L^{-1} which suggests no dimerization or oligomerization of the complexes within this concentration range.

The phosphorescence emission spectra of all these complexes except **1j**, **1h** and **1i** are illustrated in Fig. 3. As shown, excitation of these complexes in CH_2Cl_2 solution (10^{-5} M) at room temperature results in yellow luminescence. The emission maxima of **1a**–**1d** varies from 573 nm to 554 nm, which are affected by the electron-donating ability of the *para*-substituent on the phenylacetylide ligand in the order (λ_{max}, nm) of BuO > SAc > H > NO_2. The effects of the π-conjugated length of the oligo phenylacetylide ligands upon the emission of [(C^N^N)Pt(C≡$CC_6H_4)_n$-R] have been investigated. When the phenylacetylide ligand extended from ethynylbenzene monomer (**1a**) to phenylene ethynylene trimer (**1j**), the absorption maxima of the broad ^{1}MLCT transition band of **1a**, **1f** and **1j** red-shifted from 440 to 449 nm, while the corresponding emission λ_{max} slightly red-shifts from 566 to 577 nm (Fig. 4). The emission quantum yields of these three complexes are comparable, which were found in the order of **1j** > **1f** > **1a**. Complexes **1g**, **1i** and

Table 3
Spectroscopic data[a] of complexes **1a**–**1k**.

Complex	Absorption	Emission
	λ_{max}/nm	λ_{max}/nm
	(ε/× 10^3 dm^3 mol^{-1} cm^{-1})	(Φ^b)
1a	286 (60.3), 338 (19.4), 372 (13.3), 440 (8.5)	566 (0.11)
1b	292 (69.6), 373 (16.6), 443 (10.5)	567 (0.13)
1c	288 (49.7), 340 (28.9), 378 (34.7), 431 (20.7)	554 (0.19)
1d	283 (72.9), 339 (22.8), 377 (11.9), 457 (7.1)	573 (0.08)
1e	292 (48.5), 372 (14.4), 448 (9.3)	551 (0.10)
1f	285 (36.4), 339 (47.8), 446 (9.9)	568 (0.12)
1g	290 (62.9), 324 (52.9), 443 (9.3)	No emission
1h	294 (76.3), 370 (15.2), 450 (9.5)	575 (0.08)
1i	289 (58.8), 329 (55.4), 450 (8.3)	No emission
1j	294 (44.6), 343 (56.7), 449 (8.9)	577 (0.15)
1k	285 (57.8), 335 (34.0), 455 (4.5)	No emission

[a] Measured in degassed CH_2Cl_2 solutions at 298 K (1×10^{-5} mol L^{-1}).
[b] $[Ru(bpy)_3](PF_6)_2$ in degassed acetonitrile at 298 K ($\Phi_\Gamma = 0.062$) as reference.

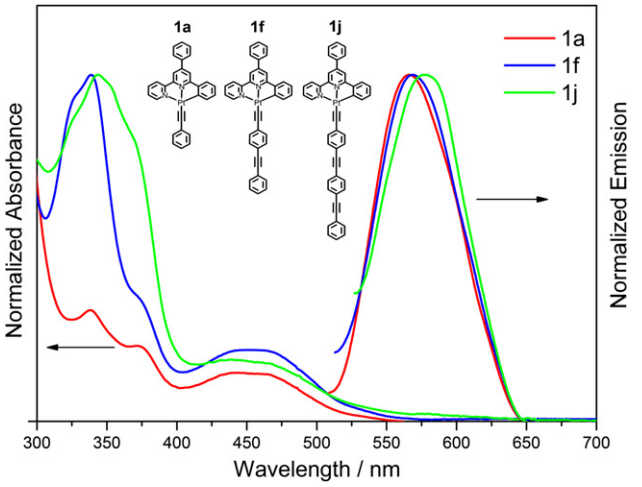

Fig 4. Normalized UV–vis absorption and emission ($\lambda_{ex} = 350$ nm) spectra of complexes **1a**, **1f** and **1j** in CH_2Cl_2 solution (10^{-5} M).

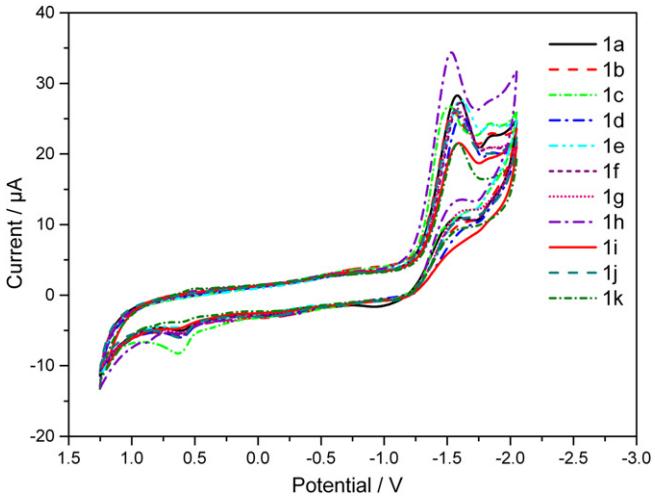

Fig 5. Cyclic voltammetry of Pt(II) complexes in CH_2Cl_2 solution.

1k have no apparent emission observed from 500 to 600 nm in their PL spectra. With reference to earlier work [12], this presumably indicates an additional non-radiative decay pathway, namely PET (photo-induced electron transfer), occurs in these complexes. The diphenylamino or butoxy unit in each of these complexes acts as an electron donor to quench the radiative pathway.

3.4. Electrochemical properties

The electrochemical behaviors of the Pt(II) complexes were investigated by cyclic voltammetry (CV) (Fig. 5) and the data are listed in Table 4. In general, the cyclic voltammograms in CH_2Cl_2 solutions at 298 K exhibit one reversible reduction couple with $E_{1/2}$ in the range of −1.52 to −1.61 V versus $Cp_2Fe^{+/0}$; this couple presumably corresponds to the one-electron reduction of the (C^N^N) ligand [13,27]. The electro-donating groups on the *para*-position of the phenylacetylide ligand shift the reduction waves to more negative direction. The electron-donating butoxy group in complex **1d** shifts the reduction wave to −1.60 V, while this reduction occurs at −1.52 V for complex **1b** which has an electron-withdrawing nitro group on the *para*-position of the phenylacetylide ligand. The conjugation length of the oligo phenylacetylide ligand does not significantly affect the (C^N^N) reduction. All complexes show an irreversible oxidation wave at 0.60–0.64 V, which can be tentatively assigned to a $Pt^{II/III}$ process [15].

Table 4
Electrochemistry data[a] of complexes **1a**–**1k**.

Complex	Oxidation E_{pa} (V)[b]	Reduction $E_{1/2}$ (V)[c]
1a	0.62	−1.55, −1.84[d]
1b	0.64	−1.56, −1.85[d]
1c	0.63	−1.52, −1.83[d]
1d	0.61	−1.61, −1.85[d]
1e	0.60	−1.60, −1.84[d]
1f	0.61	−1.60, −1.83[d]
1g	0.60	−1.58, −1.85[d]
1h	0.61	−1.53, −1.83[d]
1i	0.61	−1.59, −1.82[d]
1j	0.61	−1.56
1k	0.60	−1.59

[a] Determined in CH_2Cl_2 at 298 K with 0.1 mol L^{-1} $^nBu_4NClO_4$ as supporting electrolyte; scanning rate: 100 mV s^{-1}; Value versus $E_{1/2}(Cp_2Fe^{+/0})$ [0.11–0.13 V versus $Ag/AgNO_3$ (0.1 M in CH_3CN) reference electrode].
[b] E_{pa} refers to the anodic peak potential for the irreversible oxidation waves.
[c] $E_{1/2} = (E_{pa} + E_{pc})/2$; E_{pa} and E_{pc} are peak anodic and peak cathodic potentials, respectively.
[d] Irreversible under experimental conditions.

4. Conclusions

In summary, a series of mononuclear platinum(II) 6-phenyl-[2,2′]bipyridinyl acetylide complexes were synthesized and characterized by UV–vis absorption, phosphorescence emission spectroscopy and cyclic voltammetry. The UV absorption and PL emission maxima of these complexes are red-shifted in accordance with the electron-donating ability of the *para*-substituent on the phenylacetylide ligand. Furthermore, they also red-shift with the extension of the π-conjugated length of the oligo phenylacetylide ligands, although the differences are minor. We hope these complexes would contribute to the application of electrophosphorescent materials in OLEDs, and also serve as a model system for investigating structure-property relationships with respect to the nonlinear optical properties of cyclometalated square-planar platinum(II) complexes.

Acknowledgment

This work was supported by the postgraduate innovation fund of Jiangsu province (2009, CX09B_141Z) and the doctor thesis innovation fund of Nanjing University of Technology (2008, BSCX200812).

References

[1] Du P, Schneider J, Li F, Zhao W, Patel U, Castellano FN, et al. Bi- and terpyridyl platinum(II) chloro complexes: molecular catalysts for the photogeneration of hydrogen from water or simply precursors for colloidal platinum? Journal of the American Chemical Society 2008;130(15):5056–8.
[2] Guo FQ, Sun WF, Liu Y, Schanze K. Synthesis, photophysics, and optical limiting of platinum(II) 4′-tolylterpyridyl arylacetylide complexes. Inorganic Chemistry 2005;44(11):4055–65.
[3] Chakraborty S, Wadas TJ, Hester H, Flaschenreim C, Schmehl R, Eisenberg R. Synthesis, structure, characterization, and photophysical studies of a new platinum terpyridyl-based triad with covalently linked donor and acceptor groups. Inorganic Chemistry 2005;44(18):6284–93.
[4] Yang QZ, Wu LZ, Wu ZX, Zhang LP, Tung CH. Long-lived emission from platinum(II) terpyridyl acetylide complexes. Inorganic Chemistry 2002;41(22):5653–5.
[5] Yam VW, Tang RP, Wong KM, Cheung KK. Synthesis, luminescence, electrochemistry, and ion-binding studies of platinum(II) terpyridyl acetylide complexes. Organometallics 2001;20(22):4476–82.
[6] Hill MG, Bailey JA, Miskowski VM, Gray HB. Spectroelectrochemistry and dimerization equilibria of chloro(terpyridine)platinum(II). Nature of the reduced complexes. Inorganic Chemistry 1996;35(16):4585–90.
[7] Jarosz P, Lotito K, Schneider J, Kumaresan D, Schmehl R, Eisenberg R. Platinum (II) terpyridyl-acetylide dyads and triads with nitrophenyl acceptors via a convenient synthesis of a boronated phenylterpyridine. Inorganic Chemistry 2009;48(6):2420–8.
[8] Du P, Schneider J, Jarosz P, Zhang J, Brennessel WW, Eisenberg R. Photoinduced electron transfer in platinum(II) terpyridyl acetylide chromophores: reductive and oxidative quenching and hydrogen production. Journal of Physical Chemistry B 2007;111(24):6887–94.
[9] Schull TL, Kushmerick JG, Patterson CH, George C, Moore MH, Pollack SK, et al. Ligand effects on charge transport in platinum(II) acetylides. Journal of the American Chemical Society 2003;125(11):3202–3.
[10] Ji ZQ, Li YJ, Sun WF. 4′-(5‴-R-pyrimidyl)-2,2′:6′2″-terpyridyl (R = H, OEt, Ph, Cl, CN) platinum(II) phenylacetylide complexes: synthesis and photophysics. Inorganic Chemistry 2008;47(17):7599–607.
[11] Wang Q, Xiong F, Morlet-Savary F, Li S, Li Y, Fouassier JP, et al. Photophysical properties of cyclometalated Pt(II) complexes attached with pyrene by C–C single bond. Journal of Photochemistry and Photobiology A: Chemistry 2008;194(2–3):230–7.
[12] Qiu D, Wu J, Xie Z, Cheng Y, Wang L. Synthesis, photophysical and electrophosphorescent properties of mononuclear Pt(II) complexes with arylamine functionalized cyclometalating ligands. Journal of Organometallic Chemistry 2009;694(5):737–46.
[13] Lu W, Mi BX, Chan MCW, Hui Z, Che CM, Zhu N, et al. Light-emitting tridentate cyclometalated platinum(II) complexes containing σ-alkynyl auxiliaries: tuning of photo- and electrophosphorescence. Journal of the American Chemical Society 2004;126(15):4958–71.

[14] Wei Lu, Mi BX, Chan MCW, Hui Z, Zhu N, Lee ST, et al. [(C^N^N)Pt(C≡C)$_n$R] (HC^N^N = 6-aryl-2,2′-bipyridine, n = 1–4, R = aryl, $SiMe_3$) as a new class of light-emitting materials and their applications in electrophosphorescent devices. Chemical Communications 2002;3:206–7.
[15] Schneider J, Du P, Jarosz P, Lazarides T, Wang X, Brennessel WW, et al. Cyclometalated 6-phenyl-2,2′-bipyridyl (CNN) platinum(II) acetylide complexes: structure, electrochemistry, photophysics, and oxidative- and reductive- quenching studies. Inorganic Chemistry 2009;48(10): 4306–16.
[16] Baik C, Han WS, Kang Y, Kang SO, Ko J. Synthesis and photophysical properties of luminescent platinum(II) complexes with terdentate polypyridine ligands: [Pt(bpqb)X] and [Pt(tbbpqpy)X](PF_6) (bpqb-H = 1,3-bis(4′-phenyl-2′- quinolinyl) benzene; tbbpqpy = 4- *tert*-butyl-1,3-bis(4′-phenyl-2′-quinolinyl) pyridine; X = Cl, C≡CC_6H_5, C≡C$C_6H_4NMe_2$, C≡C$C_6H_4NO_2$. Journal of Organometallic Chemistry 2006;691(26):5900–10.
[17] Du P, Knowles K, Eisenberg R. A homogeneous system for the photogeneration of hydrogen from water based on a platinum(II) terpyridyl acetylide chromophore and a molecular cobalt catalyst. Journal of the American Chemical Society 2008;130(38):12576–7.
[18] Du P, Schneider J, Jarosz P, Eisenberg R. Photocatalytic generation of hydrogen from water using a platinum(II) terpyridyl acetylide chromophore. Journal of the American Chemical Society 2006;128(24):7726–7.
[19] Shao P, Li YJ, Sun WF. Cyclometalated platinum(II) complex with strong and broadband nonlinear optical response. Journal of Physical Chemistry A 2008;112(6):1172–9.
[20] Flatt AK, Yao Y, Maya F, Tour JM. Orthogonally functionalized oligomers for controlled self-assembly. Journal of Organic Chemistry 2004;69(5):1752–5.
[21] Maya F, Chanteau SH, Cheng L, Stewart MP, Tour JM. Synthesis of fluorinated oligomers toward physical vapor deposition molecular electronics candidates. Chemistry of Materials 2005;17(6):1331–45.
[22] Serwinski PR, Lahti PM. Limits of delocalization in through-conjugated dinitrenes: aromatization or bond formation? Organic Letters 2003;5(12):2099–102.
[23] Görl C, Alt HG. Influence of the *para*-substitution in bis(arylimino)pyridine iron complexes on the catalytic oligomerization and polymerization of ethylene. Journal of Organometallic Chemistry 2007;692(21):4580–92.
[24] Hwang JJ, Tour JM. Combinatorial synthesis of oligo(phenylene ethynylene)s. Tetrahedron 2002;58(52):10387–405.
[25] Jian H, Tour JM. Preparative fluorous mixture synthesis of diazonium- functionalized oligo(phenylene vinylene)s. Journal of Organic Chemistry 2005;70 (9):3396–424.
[26] Sheldrick GM. SHELXL-97. Program for the Refinement of Crystal Structures. Germany: University of Göttingen; 1997.
[27] Liu S, Wang Q, Jiang P, Liu R, Song GL, Zhu HJ, et al. Dyes and Pigments 2010;85(1–2):51–6.